Electronic Functions at nano-scale Level Research Team

Team Leader : Maki Kawai

Unpublished results are not included.

Reversible control of hydrogenation of a single molecule

S. Katano, Y. Kim, M. Hori, M. Trenary, M. Kawai, *Science* 316 (2007) 1883.

Low-temperature scanning tunneling microscopy was used to selectively break the N-H bond of a methylaminocarbyne ($CNHCH_3$) molecule on a Pt(111) surface at 4.7 kelvin, leaving the C-H bonds intact, to form an adsorbed methylisocyanide molecule ($CNCH_3$). The methylisocyanide product was identified through comparison of its vibrational spectrum with that of directly adsorbed methylisocyanide as measured with inelastic electron tunneling spectroscopy. The $CNHCH_3$ could be regenerated in situ by exposure to hydrogen at room temperature. The combination of tip-induced dehydrogenation with thermodynamically driven hydrogenation allows a completely reversible chemical cycle to be established at the single-molecule level in this system. By tailoring the pulse conditions, irreversible dissociation entailing cleavage of both the C-H and N-H bonds can also be demonstrated.

The investigation provides a model system for future studies of surface reaction mechanisms and may lead to new routes for fabricating nanostructures for use in molecular electronics.

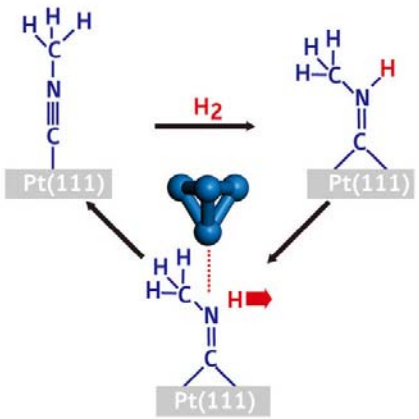

Fig 1. Reaction scheme between $CNHCH_3$ and $CNCH_3$ on Pt(111) established in this study.

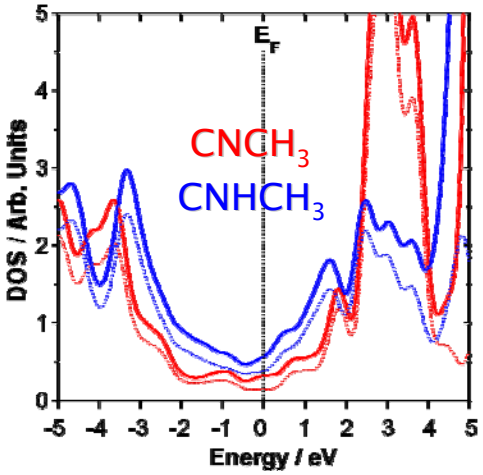

Fig 2. Calculation result showing difference in electrical conductivity between two molecules

Single-molecule reaction and manipulation by vibrational excitation with STM

M. Ohara, Y. Kim, S. Yanagisawa, Y. Morikawa, M. Kawai,
***Phys. Rev. Lett.* 100 (2008) 136104.**
M. Ohara, Y. Kim, M. Kawai, *Phys. Rev.* B 78 (2008) 201405(R).

We have elucidated how molecules of CH3S–SCH3 on a Cu(111) surface split into two CH3S fragments, and found that vibrations in the carbon–hydrogen bond, induced by an STM electron, could drive the reaction [Figs 1 and 2]. We also found that a single molecule in a vibrationally excited state on a surface can be delivered precisely to a desired position with the aid of a local electric field in a STM junction. An individual CH3S molecule hops laterally to move away from a negatively charged STM tip and to come toward a positively charged tip when the lateral hopping motion is induced by inelastically tunneled electrons and the molecule is positioned in an inhomogeneous electric field [Figs 3 and 4].

The investigation provides a model system for future studies of surface reaction mechanisms and may lead to new routes for fabricating nanostructures for use in molecular electronics.

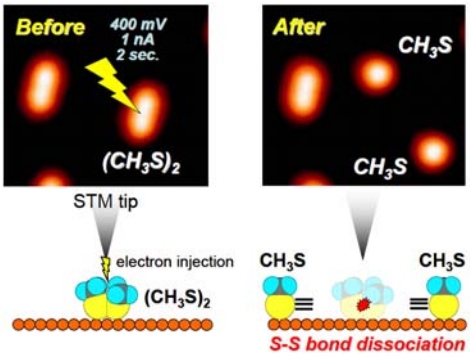

Fig 1. Topographic STM images of $(CH_3S)_2$ molecules on Cu (111) before and after injection of tunneling electrons.

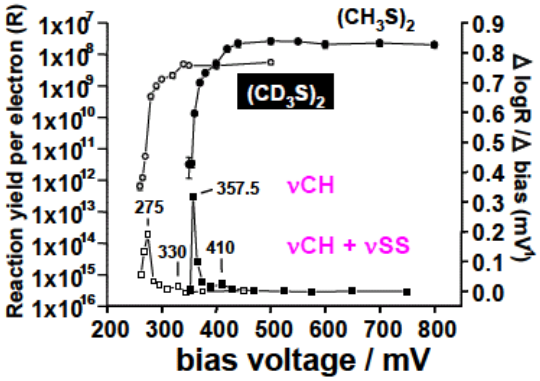

Fig 2. Action spectra showing dissociation mechanism of $(CH_3S)_2$.

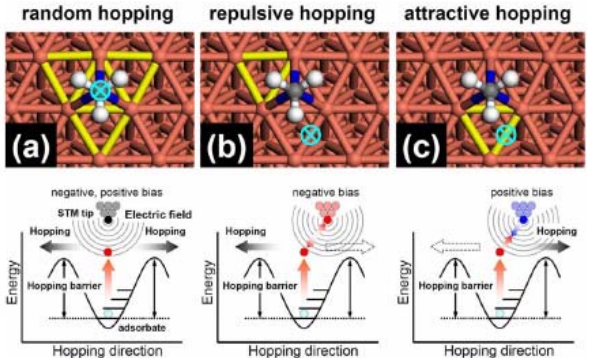

Fig 3. Schematic drawing showing controlled hopping of individual CH_3S molecules with STM.

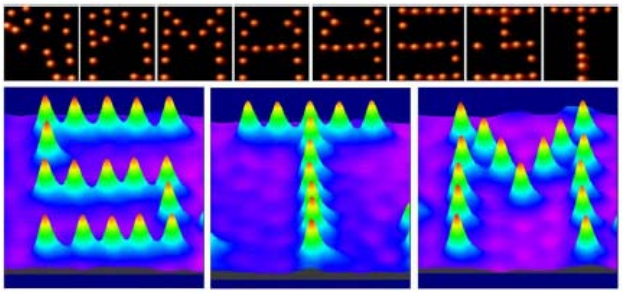

Fig 4. Sequential STM images showing the gradual construction of the letters and three-dimensional images of the letters S, T, and M with CH3S molecules on Cu(111).

Adsorption-Induced Switching of Magnetic Anisotropy in a Single Iron(II) Phthalocyanine Molecule on an Oxidized Cu(110) Surface

N. Tsukahara, K. Noto, M. Ohara, S. Shiraki, Y. Takata, J. Miyawakai, M. Taguchi, A. Chainani, S. Shin, N. Takagi and M. Kawai, *Phys. Rev. Lett.* 102 (2009) 167203.

We examined the zero-field splitting of an iron(II) phthalocyanine (FePc) attached to clean and oxidized Cu(110) surfaces and the dependence on an applied magnetic field by inelastic electron tunneling spectroscopy with STM. The symmetry of the ligand field surrounding the Fe atom is lowered on the oxidized surface, switching the magnetic anisotropy from the easy plane of the bulk to the easy axis. The zero-field splitting was not observed for FePc on a clean Cu(110) surface, and the spin state converts from triplet to singlet due to the strong coupling of Fe d states with the Cu substrate, as is also confirmed by photoelectron spectroscopy. These findings demonstrate the importance of coupling at the molecule-substrate interface for manipulating the magnetic properties of adsorbates.

These findings open the possibility of manipulating the magnetic properties of adsorbates by tuning the coupling at the molecule-substrate interface.

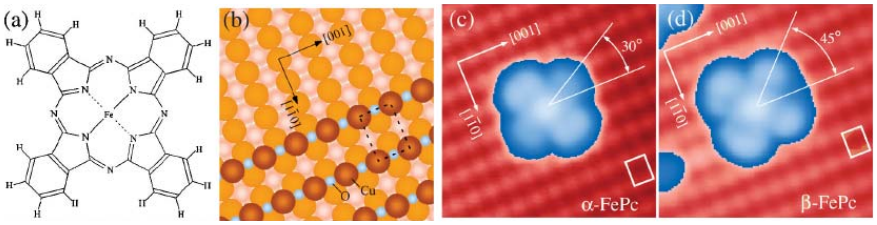

Fig 1. Schematic model of a (a) FePc molecule and (b) Cu(110)(2 x 1)-O added-row structure, and topographic STM images of (c) α- and (d) β-FePc on Cu(110)(2 x 1)-O

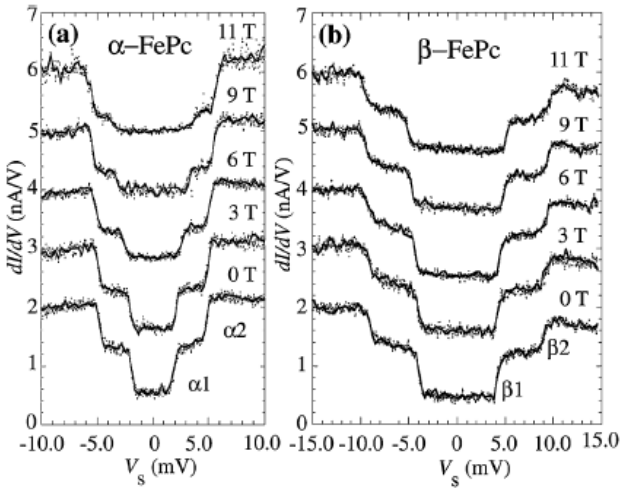

Fig 2. The dI=dV spectra of (a) α- and (b) β-FePc on Cu(110)(2 x 1)-O taken as a function of Bz (0~11 T) applied perpendicularly to the sample surface.

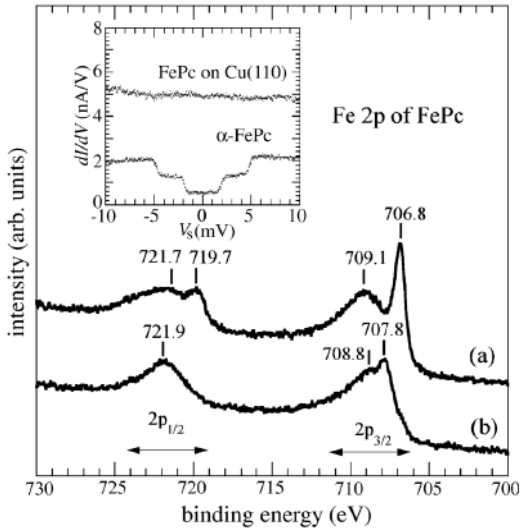

Fig 3. Fe 2p spectra of a FePc monolayer on (a) Cu(110) and (b) Cu(110)(2 x 1)-O surfaces. The inset shows the dI=dV spectra of FePc on Cu(110) and Cu(110)(2 x 1)-O at Bz = 0.

Luminescence from molecules on a metal surface excited by tunneling electrons

D. Ino, T. Yamada, M. Kawai, *J. Chem. Phys.* 129 (2008) 14701.

The electronic excitations induced with tunneling electrons into adlayers of 3,4,9,10-perylenetetracarboxylic dianhydride (PTCDA) on Ag(111) have been investigated by in situ fluorescence spectroscopy in STM. A minute area of the surface is excited by an electron tunneling process in STM. Fluorescence spectra strongly depend on the coverage of PTCDA on Ag(111). The adsorption of the first PTCDA layer quenches the intrinsic surface plasmon originated from the clean Ag(111). When the second layer is formed, fluorescence spectra are dominated by the signals from PTCDA, which are interpreted as the radiative decay from the manifold of first singlet excited state of adsorbed PTCDA. The fluorescence of PTCDA is independent of the bias polarity. In addition, the fluorescence excitation spectrum agrees with that by optical excitation. Both results indicate that S1 is directly excited by the inelastic impact scattering of electrons tunneling within the PTCDA adlayer.

The lateral localization of tunneling electrons enables us to observe the fluorescence from the short-lived excited state of adsorbed molecules. The excitation mechanism of adsorbate will help in opening up new physicochemical processes on surfaces.

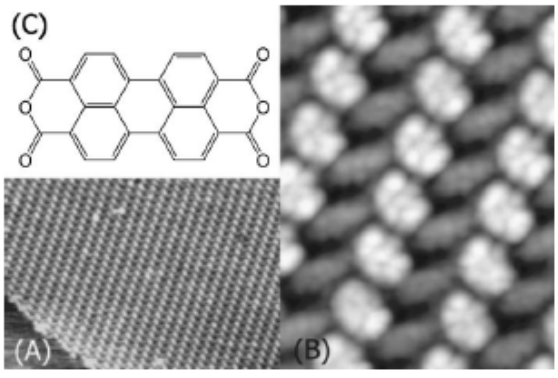

Fig 1. (a) STM image of an island of PTCDA on Ag(111). (b) STM image of a monolayer PTCDA island. (c) Chemical structure of PTCDA.

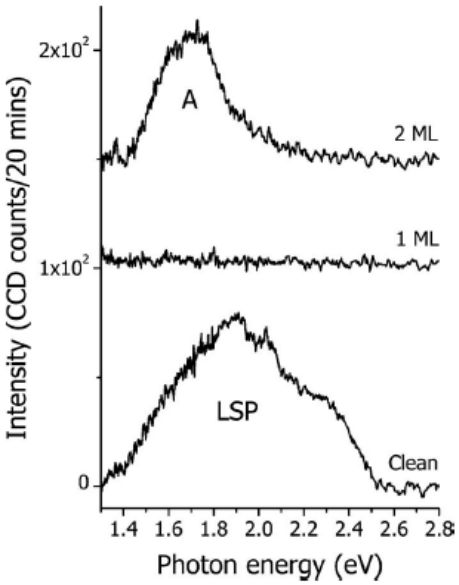

Fig 2. In situ luminescence spectra obtained from PTCDA covered Ag(111) for 1 ML, 2 ML, and the clean surface.

Hierarchical Chiral Framework Based on a Rigid Adamantane Tripod on Au(111)

S. Katano, Y. Kim, H. M, T. Kitagawa, and M. Kawai,
***J. Am. Chem. Soc.* 129 (2007) 2511, *Jpn. J. Appl. Phys.* 47 (2008) 6156.**

We have investigated the tripod-shaped bromo adamantane trithiol (BATT) molecule on Au(111) using scanning tunneling microscopy (STM) at 4.7 K. Adsorption of BATT leads to formation of highly ordered self-assembled monolayers (SAMs) with three-point contacts on Au(111). The structure of these SAMs has been found to have a two-tiered hierarchical chiral organization. The self-assembly of achiral monomers produces chiral trimers, which then act as the building blocks for chiral hexagonal supermolecules. SAMs begin to form from the racemic mixture of assembled molecules in ribbon-shaped islands, followed by the transformation to enantiomeric domains when SAM layers develop two-dimensionally across hcp domains. Such a chiral phase transition at the two-dimensional domain can arise from a subtle balance between molecule-substrate and intermolecular interactions. Two structural factors, the S atom (stabilization) and the methylene groups (chirality) located just above the S atom, induce the chiral ordering of BATT on Au(111).

Modification of surfaces by chiral molecules opens a promising path to develop biosensors at the single molecule level.

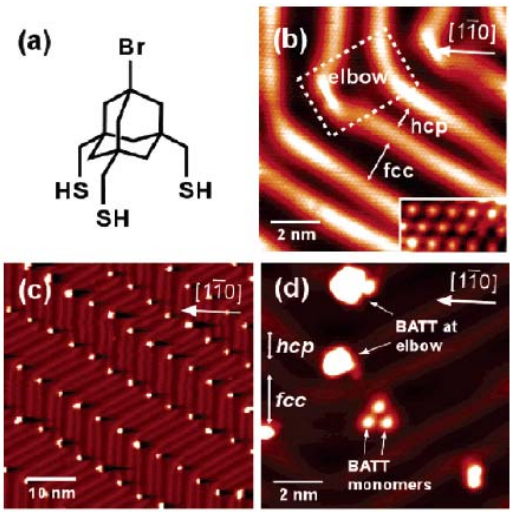

Fig 1. Schematic model of bromo adamantane trithiol (BATT) and STM images of the molecules on Au(111)

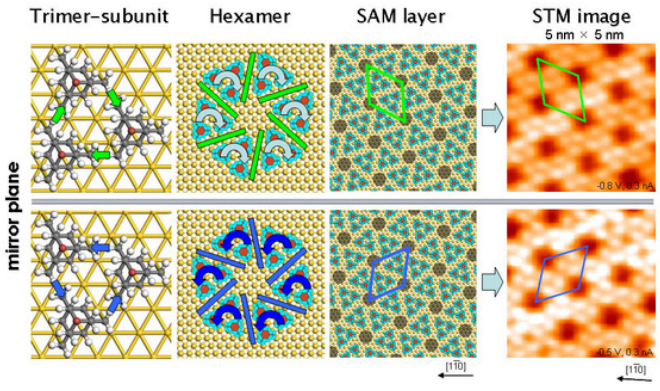

Fig 2. Views of the hierarchical chiral assembly of the adamantane derivative on a gold surface—from molecule to microscopy.

Selective Chain Reaction Leading to the Successive Growth of Molecular Lines on the Si(100)-(2×1)-H Surface

Md. Z. Hossain, H.S. Kato, M. Kawai,
***J. Phys. Chem. C* 113 (2009) 10751, *J. Am. Chem. Soc.* 130 (2008) 11518,**
***J. Am. Chem. Soc.* 129 (2007) 3328, *J. Am. Chem. Soc.* 129 (2007) 12304.**

The successive growth of mutually perpendicular molecular lines from one dangling-bond (DB) site on the Si(100)-(2x1)-H surface has been realized through a substrate-mediated chain reaction at 300 K. Among various molecules, acetone molecules undergo the most facile chain reaction with a DB site, which proceeds selectively on the Si(100)-(2x1)-H surface, resulting in only single molecular lines in the parallel-row (parallel to the dimer row) direction. The smaller size and higher reactivity of acetone molecules enable us to successively grow a parallel-row acetone line from the end of a cross-row (perpendicular to the dimer row) allylmercaptan line simply by changing the feed of gas molecules into the reaction chamber. Since the length of a molecular line is controlled by the number of gas molecules impinged, it is possible to turn a chain reaction from the cross-row direction to the parallel-row direction at any desired point on the surface. The reaction path of the adsorbing molecules is discussed. The present study provides a new means of fabricating mutually perpendicular molecular lines through a chain reaction initiating at a preselected DB site on the Si(100)-(2x1) surface.

The ability to form molecular arrays with carefully controlled geometries on a material around which the semiconductor industry revolves could have significant implications for the rapidly developing field of molecular electronics.

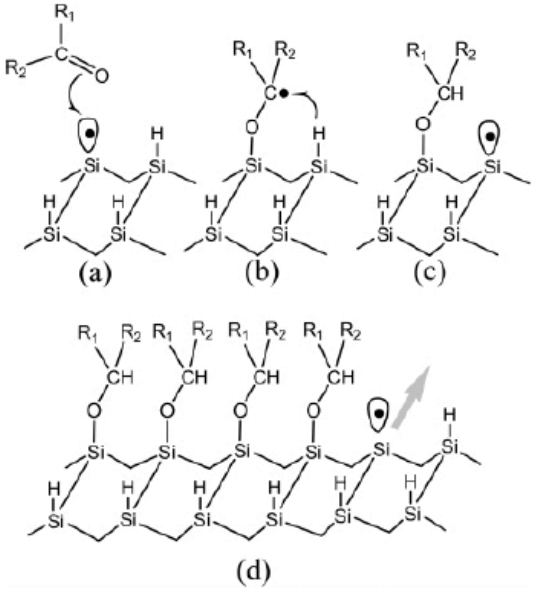

Fig 1. Schematics of chain reaction mechanism of a molecule on the Si(100)-(2x1)-H surface.

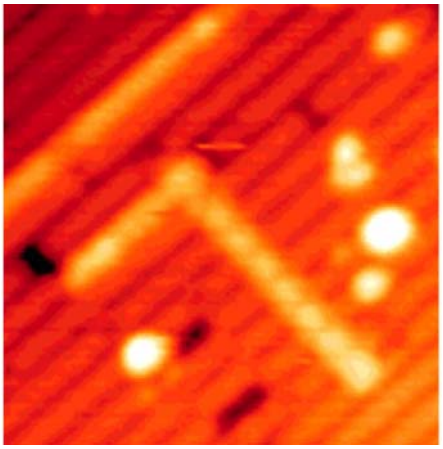

Fig 2. STM image of continuous molecular lines on Si(100)-(2x1)-H.

Modification of electronic structure of single-walled carbon nanotubes on the surface

H.-J. Shin, S. Clair, Y. Kim, M. Kawai,
***Appl. Phys. Lett.* 93 (2008) 233104, *Nature Nanotech*. 4 (2009) 567.**

We have studied the strong influence of substrates on the electronic structure of SWCNTs by means of STM. We found that the electronic properties of SWCNTs can be strongly influenced by the way the tubes are registered on metal substrates. When the amount of charge transfer is not homogeneous along the tube axis due to the commensuability beteween the tube and substrate, the SWCNT manifests periodic modulations both in topography and the electronic structure. This can give rise to quantum confinements in the form of periodic quantum-well structures over the whole length of a SWCNT [Figs1 and 2]. We also found that the work function difference between the tube and the substrate determines the direction of the Fermi level shift on the metal surface, while the electric field resulting from the dipole moment formed at the interface between the insulating film and the metal determines Fermi level for the SWCNT on insulating films [Fig 3].

The investigation provides a model system for future studies of carbon nanotubes and may lead to new routes for molecular electronics.

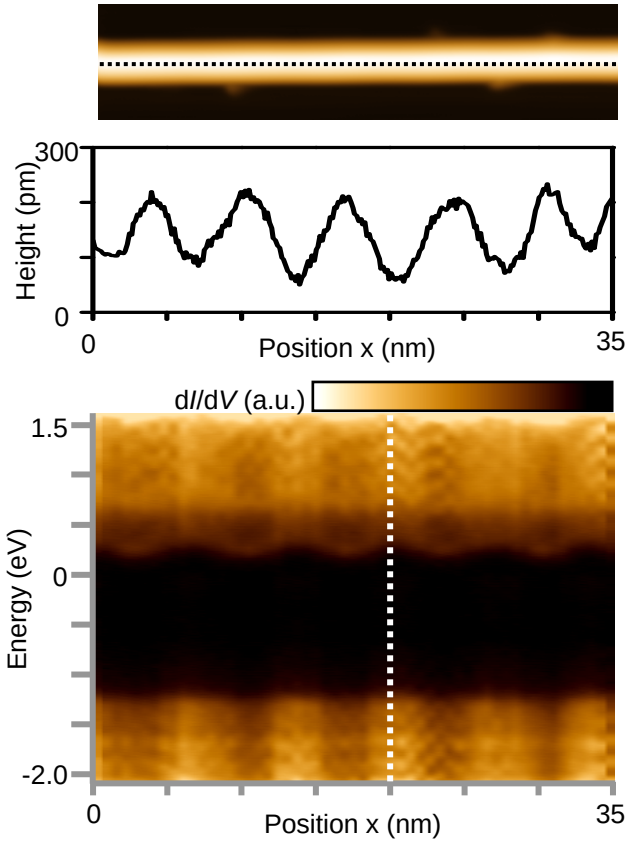

Fig 1. Periodic modulation of geometric and electronic structures in a SWCNT on Ag(100)

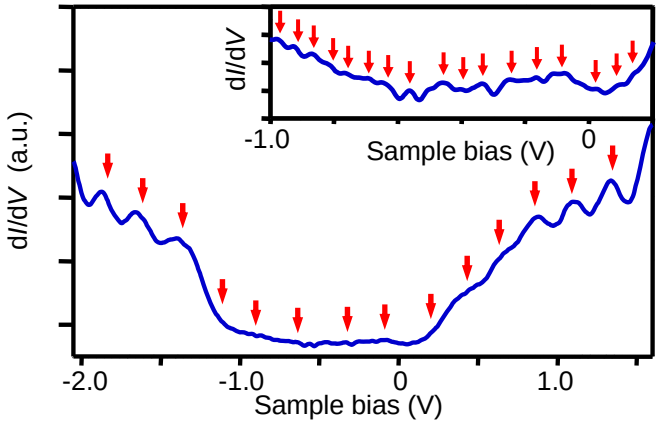

Fig 2. A differential conductance spectrum of quantum dots in a SWCNT.

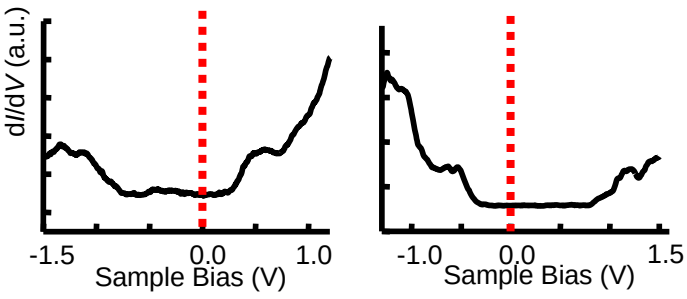

Fig 3. The dI/dV spectra of SWCNT on Ag(100) (left) and on NaCl/Ag(100) (right).

Electronic state analysis of charge transport mechanism in DNA duplexes

H.S. Kato, M. Furukawa, M. Kawai, M. Taniguchi, T. Kawai, T. Hatsui, N. Kosugi, *Phys. Rev. Lett.* 93 (2004) 086403.

M. Furukawa, H.S. Kato, M. Taniguchi, T. Kawai, T. Hatsui, N. Kosugi, T. Yoshida, M. Aida, M. Kawai, *Phys. Rev. B* 75 (2007) 045119.

The electronic state analysis has been performed for understanding of charge transport mechanism in DNA duplexes [Fig. 1]. By the antecedent analysis, the charge hopping between localized electronic states of DNA bases was proposed as a dominant process of long-range charge transport in DNA, rather than the charge transfer in delocalized states [Fig. 2]. The origin of conductivity increase at the chemical carrier dope, in addition, has been characterized to be the modification of electronic states near the Fermi level of DNA as the way of conductive polymers [Fig. 3].

The understanding of electronic states of nano-structural materials, such as DNA, is important to utilize them for future molecular devices and to synthesis new functional molecules, in both of chemical and biochemical aspects.

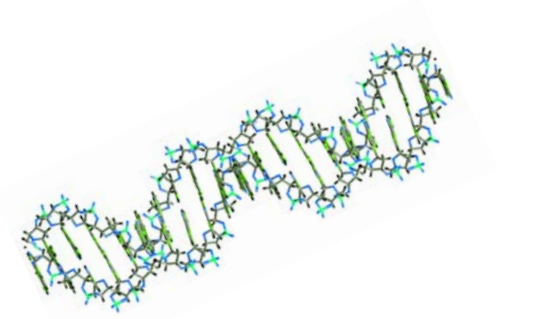

Fig 1. Schematic view of a DNA duplex.

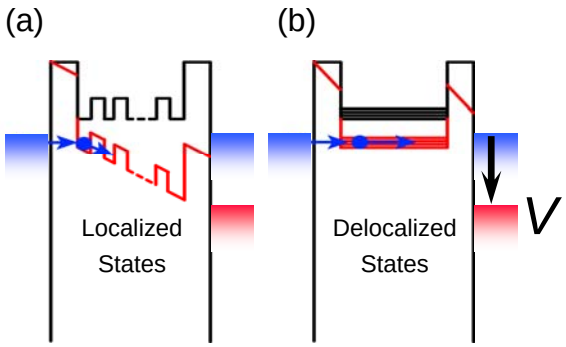

Fig 2. Antithetical models of charge transport in DNA duplexes: (a) charge hopping model with localized states, and (b) charge transfer model with delocalized states.

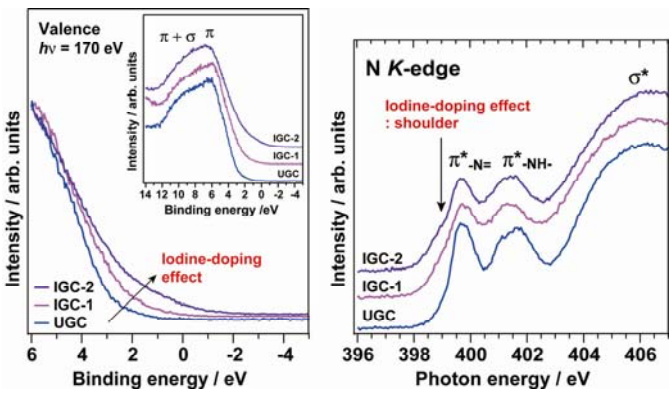

Fig 3. Change of occupied and unoccupied electronic states of DNA duplexes at the chemical carrier dope.

Visualization of Phospholipid Particle Fusion Induced by Duramycin

S. Matsunaga, T. Matsunaga, K. Iwamoto, T. Yamada, M. Shibayama, M. Kawai, T. Kobayashi, *Langmuir* 25 (2009) 8200, *Electrochem. Comm.* 9 (2007) 645.

We visualized nanometer-scale phospholipid particle fusion by STM on an alkanethiol-modified gold substrate, induced by duramycin, a tetracyclic antibiotic peptide with 19 amino residues. Ultrasonic homogenization generated a suspension mainly consisting of minimal lipid particles (MLP) from 1-palmitoyl-2-oleoyl-sn-glycero-3-phosphocholine (POPC), and 1-palmitoyl-2-oleoyl-sn-glycero-3-phosphoethanolamine (POPE) in a phosphate buffer solution, confirmed by dynamic light scattering (DLS). In situ STM discerned individual MLPas particles (diameter~8 nm) spread on Au(111), modified with alkanethiol, within the suspension. The MLP became fragile by the presence of duramycin, and the MLP were easily scratched by the scanning tip into multilayers along the surface. This process of particle fusion on the gold surface coincides with the aggregation of MLP in the suspension, observed by DLS. It was demonstrated that STM is capable of discerning and monitoring the nanometer-scale features of phospholipid particles altered by antibiotics with biochemical impact. STM might allow in situ, real-space, nanometer-scale observations of minute particles composed of phospholipids within the real cells with the highest magnification ratio.

This study shows that we can apply scanning tunneling microscope for a nanometer scale observation of bio-reactions. This technique enables use to reveal the unclear mechanism of many bio-reactions

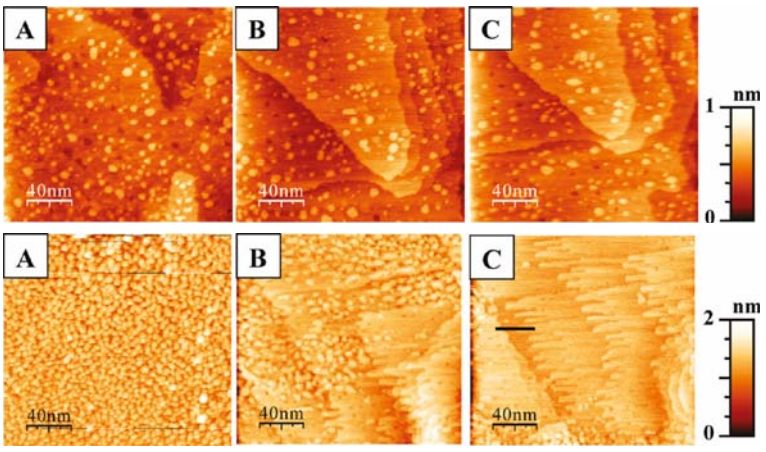

Fig 1. *In situ* STM images of POPC and POPC+POPE aggregations sitting on the substrate. A) No duramycin, B) Right after addition of 7 μM duramycin, C) 10 min. after B). In the POPE containing system, particles fused with each other.

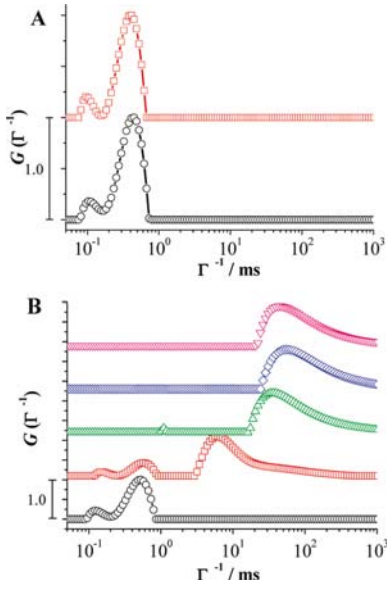

Fig 2. DLS results of A) POPC+duramycin, and B) POPC+POPE+duramycin. In the POPE containing system, small particles fused and formed large aggregations.

A Novel Mucin Extracted from Jellyfish and Application as Nanowire

A. Masuda, T. Baba, N. Dohmae, M. Yamamura, H. Wada, and K. Ushida
***Journal of Natural Products* 70 (2007) 1089.**
J. Uzawa, M. Urai, T. Baba, Hi. Seki, K. Taniguchi and K. Ushida
***Journal of Natural Products.* 72 (2009) 818.**
M. Urai, T. Nakamura, J. Uzawa, T. Baba, K. Taniguchi, H. Seki and K. Ushida
***Carboohydrate Research* 344 (2009) 2182.**

Mucin is a kind of polymeric glycoprotein having repeating peptide main chain with blanched O-glycan chains. We found a novel mucin which can be used as a raw material for nanowires. Q-mucin was extracted from various kinds of jellyfishes including world biggest one (Nomura's jellyfish) causing huge economical and social damages on Japanese coastal arias every years, therefore, its production in an industrial scale is in scope. On detailed structural analyses using NMR spectroscopy and high resolution mass spectrometry, Q-mucin has an extremely simple and well-defined structure different from general mucins which show remarkable multiplicity in glycochains and the treatment of which as a single material is impossible. We observed a ribon-like shape of Q-mucin on AFM of which length depends on its molecular mass fractionated on size exclusion chromatography.

The glycan chains has an ability of molecular recognitions with proteins as found in real biological systems. Chemical modification on the glycochain of Q-mucin is possible. Fabrication of Q-mucin as nanowire will provide various applications in industrial, medical, and biological fields as well.

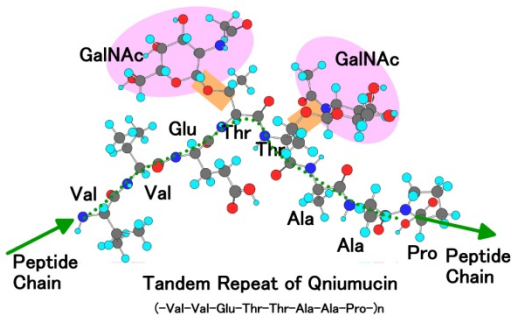

Fig 1. 3D structure of the tandem repeat part Q-mucin clarified by NMR and mass spectrometry

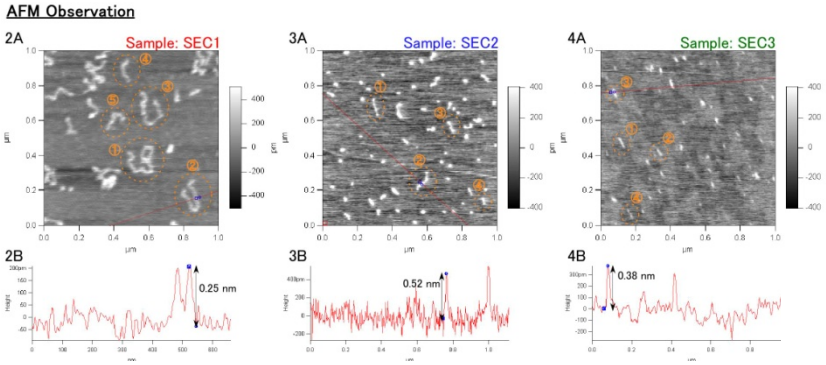

Fig 2. AFM image of Q-mucin on mica plates. The sample was fractionated by size exclusion chrmatography (SEC) The averaged molecular mass were 260, 90, and 40 kDa, and averaged length of ribbon-like images were 150-560, 40-110, and 43-82 nm for 2-4, respectively.

pH-dependent formation of membranous cytoplasmic body-like structure of ganglioside G(M1)/bis(monoacylglycero)phosphate mixed membranes.

Hayakawa T, Makino A, Murate M, Sugimoto I, Hashimoto Y, Takahashi H, Ito K, Fujisawa T, Matsuo H, Kobayashi T. Biophys J. 92, L13 (2007)

Membrane structures of the mixtures of ganglioside G(M1) and endosome specific lipid, bis (monoacylglycero) phosphate (BMP, also known as lysobisphosphatidic acid) were examined at various pH conditions by freeze-fracture electron microscopy and small-angle x-ray scattering. At pH 8.5-6.5, a G(M1)/BMP (1:1 mol/mol) mixture formed small vesicular aggregates, whereas the mixture formed closely packed lamellar structures under acidic conditions (pH 5.5, 4.6) with the lamellar repeat distance of 8.06 nm. Since BMP alone exhibits a diffuse lamellar structure at a broad range of pH values and G(M1) forms a micelle, the results indicate that both G(M1) and BMP are required to produce closely stacked multilamellar vesicles. These vesicles resemble membranous cytoplasmic bodies in cells derived from patients suffering from G(M1) gangliosidosis. Similar to G(M1) gangliosidosis, cholesterol was trapped in BMP vesicles in G(M1)- and in a low pH-dependent manner. Studies employing different gangliosides and a G(M1) analog suggest the importance of sugar chains and a sialic acid of G(M1) in the pH-dependent structural change of G(M1)/BMP membranes.

This study indicates that endosome specific lipids and glycolipids are sufficient for the alteration of lysosome structure in particular diseases. The drugs and treatments that intereracts with BMP may prevent this alteration and eventually lysosome diseases.

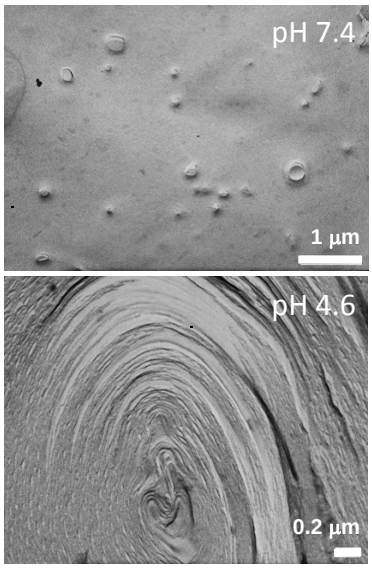

Fig 1. Freeze-fracture electron micrographs of G_{M1}/BMP (1:1 mol/mol) mixture at different pH.

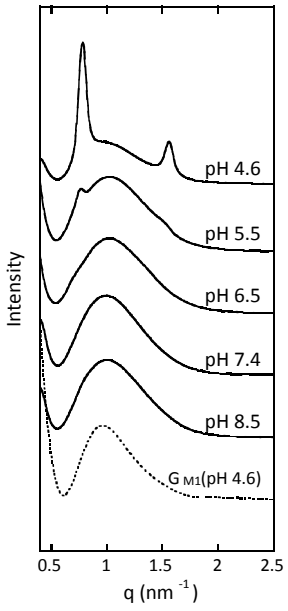

Fig 2. SAXS patterns of G_{M1} at pH 4.6 and G_{M1}/BMP mixture at different pH.

Curvature-dependent recognition of ethanolamine phospholipids by duramycin and cinnamycin.

Iwamoto K, Hayakawa T, Murate M, Makino A, Ito K, Fujisawa T, Kobayashi T.
Biophys J. 93, 1608 (2007)

Duramycin is a 19-amino-acid tetracyclic lantibiotic closely related to cinnamycin (Ro09-0198), which is known to bind phosphatidylethanolamine (PE). The lipid specificity of duramycin was not established. The present study indicates that both duramycin and cinnamycin exclusively bind to ethanolamine phospholipids (PE and ethanolamine plasmalogen). Model membrane study indicates that the binding of duramycin and cinnamycin to PE-containing liposomes is dependent on membrane curvature, i.e., the lantibiotics bind small vesicles more efficiently than large liposomes. The binding of the lantibiotics to multilamellar liposomes induces tubulation of membranes, as revealed by electron microscopy and small-angle x-ray scattering. These results suggest that both duramycin and cinnamycin promote their binding to the PE-containing membrane by deforming membrane curvature.

This study provides the molecular basis of lipid-protein interaction. The induction of tubulation of the phosphatidylethanolamine-containing membranes may be useful for the fabrication of nano-sized membranes using PE and duramycin.

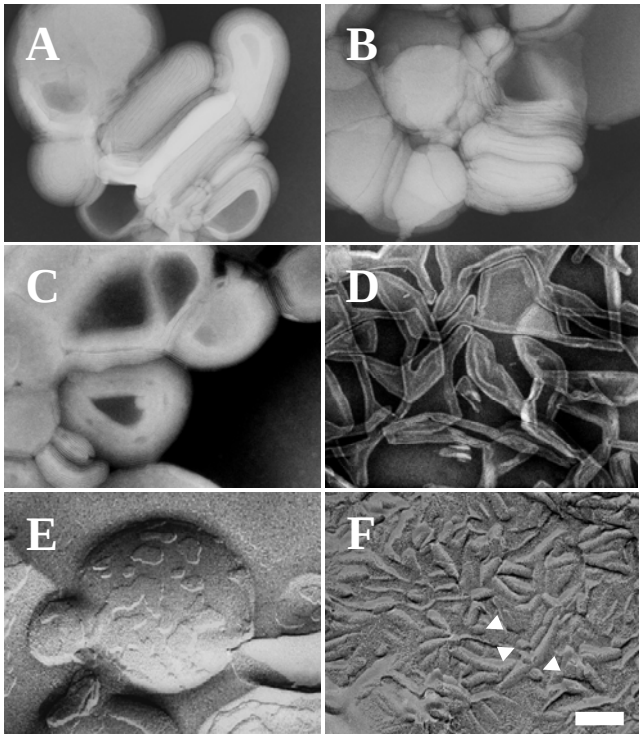

Fig 1. Duramycin deforms PE-containing membranes into a rodlike structure. Two millimolar (total lipids) MLVs composed of POPC (A, C, and E) and POPC/POPE (9:1) (B, D, and F) were incubated in the absence (A and B) or the presence (C–F) of 500 μM duramycin for 30 min at 37 °C. (A–D) Negative staining images, and (E, F) freeze fracture replica. Arrows indicate round-shape images, whose diameters were 20–25 nm. Bar, 100 nm.

δ-bonding contribution of a strong π-acceptor molecule: Surface chemical bond of SO_2 on Ni(100)

T. Tokushima, K. Sodeyama, Y. Harada, Y. Takata, M. Nagasono, Y. Kitajima, Y. Tamenori, H. Ohashi, S. Tsuneyuki, A. Hiraya, and S. Shin, Phys. Rev. B 78 (2008) 085405

The electronic structure and chemical bonding of SO_2 adsorbed on Ni(100) were investigated by means of O 1s x-ray emission spectroscopy and DFT calculations. Elemental and symmetry specificities [see Fig.1] of x-ray emission spectroscopy enable us to directly probe surface chemical bonding formed by strong hybridization of O 2p with Ni 3d orbital. The most remarkable change in adsorption is appearance of broad features near the Fermi energy of Ni. The features are assigned to the MOs originating from strong surface chemical bonding due to strong hybridization between the O 2p orbitals of SO_2 and the Ni 3d orbital [see Fig.2 and 3]. Contrary to the expected character of the SO_2 molecule as a strong π acceptor, our measurement shows that SO_2/Ni(100) system has characteristic chemical bonding which contains clear contribution of σ orbitals in addition to π orbitals.

Studies of the interaction between a molecule and a surface metal atom provides important fundamental knowledge which gives insight into surface chemistry such as elementary processes of catalytic reaction and corrosion.

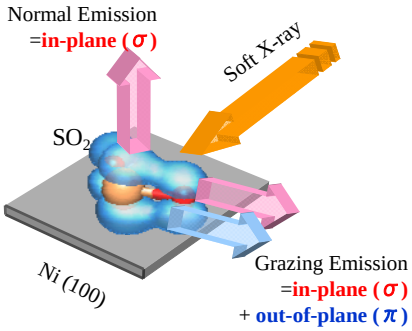

Fig 1. Schematic of emission angle dependence of XES for surface adsorbed SO_2.

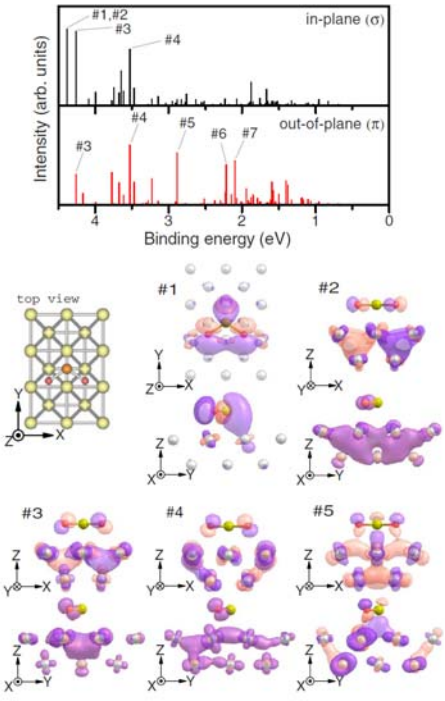

Fig 2. Assignment of calculated XES spectral features between 0–4.5 eV binding energy in terms of symmetry resolved π and δ states. MO pictures for typical peaks are also depicted.

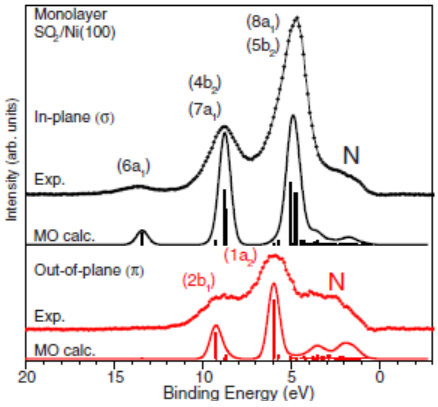

Fig 3. Simulated XES spectra of monolayer SO_2 on Ni(100) obtained by DFT calculations together with symmetry resolved XES spectra. Calculated MOs of SO_2 on Ni(100) labeled in terms of corresponding MOs of the isolated SO_2 molecule.

Out-of-plane nesting driven spin spiral in ultrathin Fe/Cu(001) films

J. Miyawaki, A. Chainani, Y. Takata, M. Mulazzi, M. Oura, Y. Senba, H. Ohashi, S. Shin

***Phys. Rev. Lett.* (accepted)**

Epitaxial ultrathin Fe films on fcc Cu(001) exhibit a spin spiral (SS), in contrast to the ferromagnetism of bulk bcc Fe. We study the in-plane and out-of-plane Fermi surfaces (FSs) of the SS in 8 monolayer Fe/Cu(001) films using energy dependent soft x-ray angle-resolved photoemission spectroscopy (ARPES). It was found that the SS originates in nested regions confined to out-of-plane FSs, which are drastically modified compared to in-plane FSs. From precise reciprocal space maps along k_z in successive Brillouin zones, we identify the associated real space compressive strain of 1.5±0.5% along *c*-axis. An autocorrelation analysis quantifies the incommensurate ordering vector $\boldsymbol{q}=(2\pi/a)(0,0,\sim0.86)$, favoring a SS. These results are consistent with magneto-optic Kerr effect and surface x-ray diffraction experiments and suggest the importance of in-plane and out-of-plane FS mapping for ultrathin films.

In-plane and out-of-plane band and FS mapping provides a new insight into the strain control of properties in ultrathin films of element, oxides, and their multilayers, heterostructures, interfaces, etc.

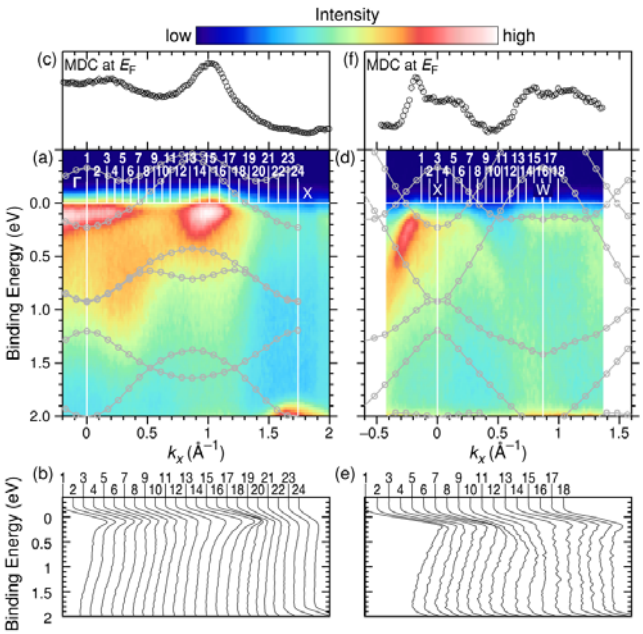

Fig. 1 ARPES results of Fe(8 ML)/Cu(001) at 50 K. (a) and (d) In-plane band maps measured at $h\nu$=430 and 580 eV. The gray lines and points are the band calculation of fcc Fe for $\boldsymbol{q}=(2\pi/a)(0.5,0,1)$ [M. Körling and J. Ergon, Phys. Rev. B 54, R8293 (1996)]. (b) and (e) EDCs at some k_x points. (c) and (f) MDCs at EF.

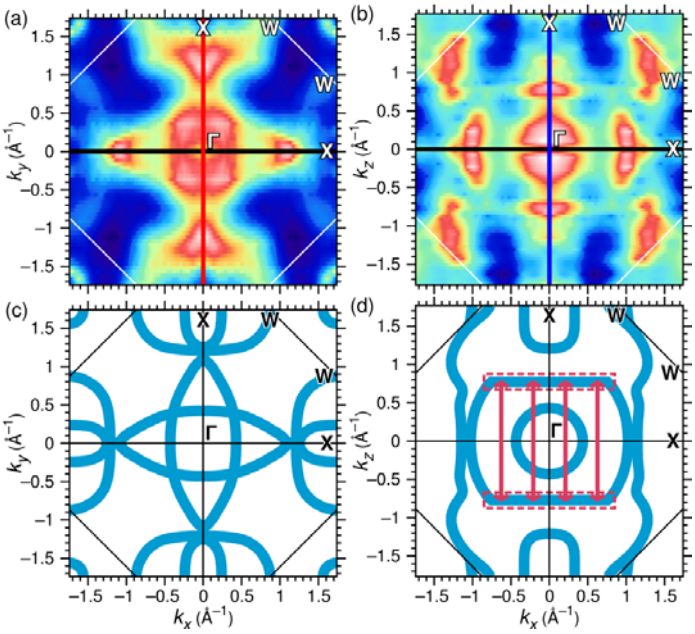

Fig 2. In-plane and out-of-plane FSs of Fe(8 ML)/Cu(001). (a) and (b) In-plane and out-of-plane FSs. (c) and (d) In-plane and out-of-plane FS crossings extracted from MDCs. The regions indicated by the red dotted lines are the nesting parts and were used for the autocorrelation analysis.